Mechanics of Blood Vessels

Thomas R. Canfield
Argonne National Laboratory
Argonne, Illinois

and

Philip B. Dobrin
Hines VA Hospital and Loyola University Medical Center
Hines, Illinois

Introduction

This chapter is concerned with the mechanical behavior of blood vessels under static loading conditions and the methods required to analyze this behavior. The assumptions underlying this discussion are for *ideal* blood vessels that are at least regionally homogeneous, incompressible, elastic, and cylindrically orthotropic. Although physiological systems are *nonideal*, much understanding of vascular mechanics has been gained through the use of methods based upon these ideal assumptions.

Homogeneity of the vessel wall. On visual inspection, blood vessels appear to be fairly homogeneous and distinct from surrounding connective tissue. The inhomogeneity of the vascular wall is realized when one examines the tissue under a lowpower microscope, where one can easily identify two distinct structures: the media and adventitia. For this reason the the assumption of vessel wall homogeneity is applied cautiously. Such an assumption may be valid only within distinct macroscopic structures. However, few investigators have incorporated macroscopic inhomogeneity into studies of vascular mechanics [17].

Incompressibility of the vessel wall. Experimental measurement of wall compressibility of 0.06% at 270 cm of H_2O indicates that the vessel can be considered incompressible when subjected to physiological pressure and load [2]. In terms of the mechanical behavior of blood vessels, this is small relative to the large magnitude of the distortional strains that occur when blood vessels are deformed under the same conditions. Therefore, vascular compressibility may be important to understanding other physiological processes related to blood vessels, such as the transport of interstitial fluid.

Inelasticity of the vessel wall. That blood vessel walls exhibit inelastic behavior such as length–tension and pressure–diameter hysteresis, stress relaxation, and creep has been reported extensively [1], [10]. However, blood vessels are able to maintain stability and contain the pressure and flow of blood under a variety of physiological conditions. These conditions are dynamic, but slowly varying with a large static component.

Residual stress and strain. Blood vessels are known to retract both longitudinally and circumferentially after excision. This retraction is caused by the relief of distending forces resulting from internal pressure and longitudinal tractions. The magnitude of retraction is influenced by several factors. Among these factors are growth, aging, and hypertension. Circumferential retraction of medium–caliber blood vessels, such as the carotid, illiac, and bracheal arteries, can exceed 70% following reduction of internal blood pressure to zero. In the case of the carotid artery, the amount of longitudinal retraction tends to increase during growth and to decrease in subsequent aging [5]. It would seem reasonable to assume that blood vessels are in a nearly stress–free state when they are fully retracted and free of external loads. This configuration also, seems to be a reasonable choice for the reference configuration. However, this ignores residual stress and strain effects that have been the subject of current research [4], [16], [11], [12], [13], [14].

Blood vessels are formed in a dynamic environment which gives rise to imbalances between the forces that tend to extend the diameter and length and the internal forces that tend to resist this extension. This imbalance is thought to stimulate the growth of elastin and collagen and to effectively reduce the stresses in the underlying tissue. Under these conditions it is not surprising that a residual stress state exists when the vessel is fully retracted and free of external tractions. This process has been called remodeling [11]. Striking evidence of this remodeling is found when a cylindrical slice of the fully retracted blood vessel is cut longitudinally through the wall. The cylinder springs open, releasing bending stresses kept in balance by the cylindrical geometry [16].

Vascular Anatomy

A blood vessel can be divided anatomically into three distinct cylidrical sections when viewed under the optical microscope. Starting at the inside of the vessel they are the intima, the media, and the adventitia. These structures have distinct functions in terms of the blood vessel physiology and mechanical properties.

The intima consists of a thin monolayer of endothelial cells that line the inner surface of the blood vessel. The endothelial cells have little influence on blood vessel mechanics, but do play an important role in hemodynamics and transport phenomena. Because of their anatomical location, these cells are subjected to large variations in stress and strain as a result of pulsatile changes in blood pressure and flow.

The media represents the major portion of the vessel wall and provides most of the mechanical strength necessary to sustain structural integrity. The media is organized into alternating layers of interconnected smooth muscle cells and elastic lamellae. There is evidence of collagen throughout the media. These small collagen fibers are found within the bands of smooth muscle and may participate in the transfer of forces between the smooth muscles cells and the elastic lamellae. The elastic lamellae are composed principally of the fiberous protein elastin. The number of elastic lamellae depends upon the wall thickness and the anatomical location [18]. In the case of the canine carotid, the elastic lamellae account for a major component of the static structural response of the blood vessel [6]. This response is modulated by the smooth muscle cells, which have the ability to actively change the mechanical characteristics of the wall [7].

The adventitia consists of loose, more disorganized fiberous connective tissue, which may have less influence on mechanics.

Axisymmetric Deformation

In the following discussion we will concern ourselves with deformation of cylindrical tubes, see Fig. 1. Blood vessels tend to be nearly cylindrical in situ and tend to remain cylindrical when a cylindrical section is excised and studied in vitro. Only when the vessel is dissected further does the geometry begin to deviate from cylindrical. For this deformation there is a unique coordinate mapping;

$$(R, \Theta, Z) \longrightarrow (r, \theta, z) \,, \tag{1}$$

where the undeformed coodinates are given by (R, Θ, Z) and the deformed coordinates are given by (r, θ, z). The deformation is given by a set of restricted functions,

$$r = r(R) \,, \tag{2}$$

$$\theta = \beta\Theta \,, \tag{3}$$

$$z = \mu Z + c_1 \ , \tag{4}$$

$$\tag{5}$$

where the constants μ and β have been introduced to account for a uniform longitudinal strain and a symmetric residual strain that are both independent of the coordinate Θ.

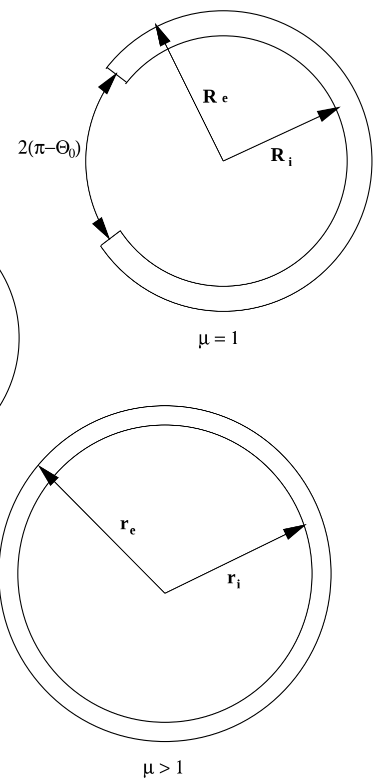

Figure 1: Cylindrical geometry of a blood vessel: *top:* stress–free' reference configuration; *middle:* fully retracted vessel free of external traction; *bottom:* vessel in situ under longitudinal tether and internal pressurization

If $\beta = 1$, there is no residual strain. If $\beta \neq 1$, residual stresses and strains are present. If $\beta > 1$, a longitudinal cut through the wall will cause the blood vessel to open up, and the new cross–section will form a c–shaped section of an annulus with larger internal and external radii. If $\beta < 1$, the cylindrical shape is unstable, but a thin section will tend to overlap itself.

In Choung and Fung's formulation, $\beta = \pi/\Theta_0$, where the angle Θ_0 is half the angle spanned by the open annular section [4].

For cylindrical blood vessels there are two assumed constraints. The first assumption is that the longitudinal strain is uniform through the wall and therefore

$$\lambda_z = \mu = \text{a constant} \tag{6}$$

for any cylindrical configuration. Given this, the principal stretch ratios are computed from the above functions as

$$\lambda_r = \frac{dr}{dR} \,, \tag{7}$$

$$\lambda_\theta = \beta \frac{r}{R} \tag{8}$$

$$\lambda_z = \mu \,. \tag{9}$$

The second assumption is wall incompressibility, which can be expressed by

$$\lambda_r \lambda_\theta \lambda_z \equiv 1 \tag{10}$$

or

$$\beta\mu \frac{r}{R}\frac{dr}{dR} = 1 \tag{11}$$

and therefore

$$r dr = \frac{1}{\beta\mu} R dR \,. \tag{12}$$

Integration of this expression yields the solution

$$r^2 = \frac{1}{\beta\mu} R^2 + c_2 \,, \tag{13}$$

where

$$c_2 = r_e^2 - \frac{1}{\beta\mu} R_e^2 \,. \tag{14}$$

As a result, the principal stretch ratios can be expressed in terms of R as follows:

$$\lambda_r = \frac{R}{\sqrt{\beta\mu(R^2 + \beta\mu c_2)}} \,, \tag{15}$$

$$\lambda_\theta = \sqrt{\frac{1}{\beta\mu} + \frac{c_2}{R^2}} \,. \tag{16}$$

Experimental Measurements

The basic experimental setup required to measure the mechanical properties of blood vessels in vitro is described in [7]. It consists of a temperature regulated bath of physiological saline solution to maintain immersed cylindrical blood vessel segments, devices to measure diameter, an apparatus to hold the vessel at a constant longitudinal extension and to measure longitudinal distending force, and a system to deliver and control the internal pressure of the vessel with 100% oxygen. Typical data obtained from this type of experiment are shown in Figs. 2 and 3.

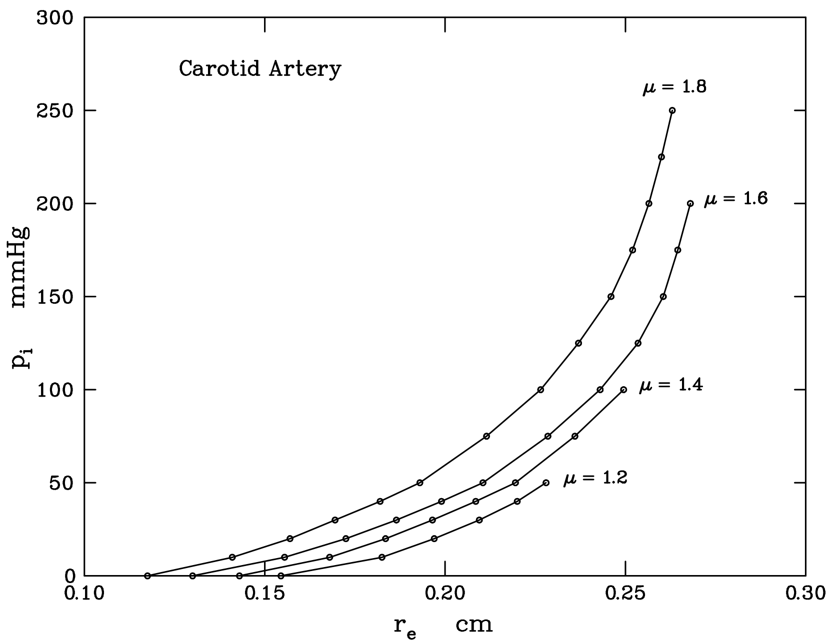

Figure 2: Pressure–radius curves for the canine carotid artery at various degrees of longitudinal extension

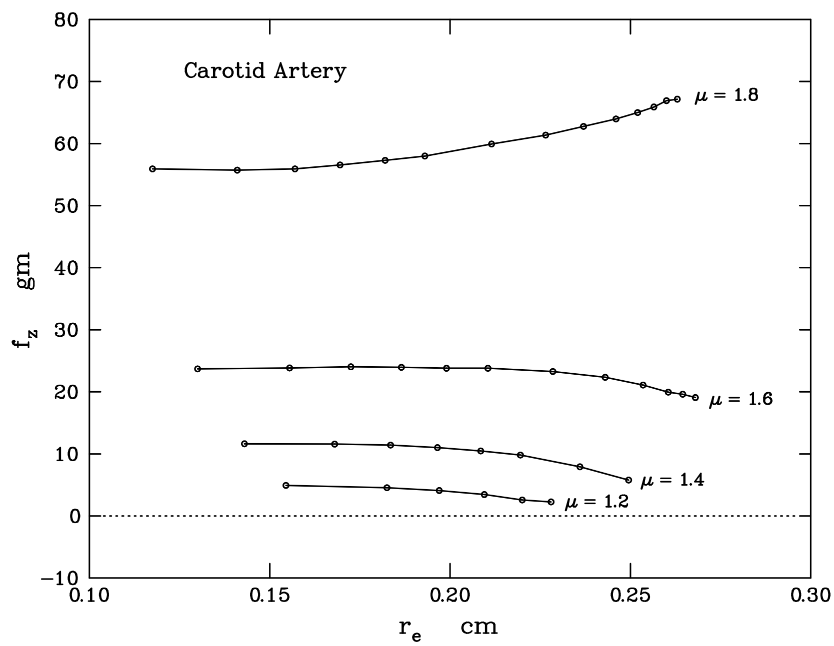

Figure 3: Longitudinal distending force as a function of radius at various degrees of longitudinal extension

Equilibrium

When blood vessels are excised, they retract both longitudinally and circumferentially. Restoration to natural dimensions requires the application of internal pressure, p_i, and a longitudinal tether force, F_T. The internal pressure and longitudinal tether are balanced by the development of forces within the vessel wall. The internal pressure is balance in the circumferential direction by a wall tension, T. The longitudinal tether force and pressure are balance by the retractive force of the wall, F_R,

$$T = p_i r_i \ , \tag{17}$$

$$F_R = F_T + p_i \pi r_i^2 \ . \tag{18}$$

The first equation is the familiar law of Laplace for a cylindrical tube with internal radius r_i. It indicates that the force due to internal pressure, p_i, must be balanced by a tensile force (per unit length), T, within the wall. This tension is the integral of the circumferentially directed force intensity (or stress, σ_θ) across the wall:

$$T = \int_{r_i}^{r_e} \sigma_\theta dr = \bar{\sigma}_\theta \, h \ , \tag{19}$$

where $\bar{\sigma}_\theta$ is the mean value of the circumferential stress and h is the wall thickness. Similarly, the longitudinal tether force, F_T, and extending force due to internal pressure are balanced by a retractive internal force, F_R, due to axial stress, σ_z, in the blood vessel wall:

$$F_R = 2\pi \int_{r_i}^{r_e} \sigma_z r dr = \bar{\sigma}_z \, \pi h(r_e + r_i) \ , \tag{20}$$

where $\bar{\sigma}_z$ is the mean value of this longitudinal stress. The mean stresses are calculated from the above equations as

$$\bar{\sigma}_\theta = p_i \frac{r_i}{h} \ , \tag{21}$$

$$\bar{\sigma}_z = \frac{F_T}{\pi h(r_e + r_i)} + \frac{p_i}{2}\frac{r_i}{h} \ . \tag{22}$$

The mean stresses are a fairly good approximation for thin walled tubes where the variations through the wall are small. However, the range of applicability of the thin–wall assumption is dependent upon the material properties and geometry. In a linear elastic material, the variation in σ_θ is less than 5% for $r/h > 20$. When the material is nonlinear or the deformation is large, the variations in stress can be more severe (see Fig. 10).

The stress distribution is determined by solving the equilibrium equation,

$$\frac{1}{r}\frac{d}{dr}(r\sigma_r) - \frac{\sigma_\theta}{r} = 0 \ . \tag{23}$$

This equation governs how the two stresses are related and must change in the cylindrical geometry. For uniform extension and internal pressurization the stresses must be functions of a single radial coordinate, r, subject to the two boundary conditions for the radial stress:

$$\sigma_r(r_i, \mu) = -p_i \ , \tag{24}$$

$$\sigma_r(r_e, \mu) = 0 \ . \tag{25}$$

Strain Energy Density Functions

Blood vessels are able to maintain their structural stability and contain steady oscillating internal pressures. This property suggest a strong elastic component, which has been called the pseudoelasticity [10]. This elastic response can be characterized by a single potential function called the strain energy density. It is a scalar function of the strains that determines the amount of stored elastic energy per unit volume. In the case of a cylindrically orthotropic tube of incompressible material, the strain energy density can be written in the following functional form:

$$W = W^*(\lambda_r, \lambda_\theta, \lambda_z) + \lambda_r \lambda_\theta \lambda_z p \ , \tag{26}$$

where p is a scalar function of position, R. The stresses are computed from the strain energy by the following:

$$\sigma_i = \lambda_i \frac{\partial W^*}{\partial \lambda_i} + p \ . \tag{27}$$

We make the following transformation [3]

$$\lambda = \frac{\beta r}{\sqrt{\beta \mu (r^2 - c_2)}} \ , \tag{28}$$

which upon differentiation gives

$$r \frac{d\lambda}{dr} = \beta^{-1}(\beta\lambda - \mu\lambda^3) \ . \tag{29}$$

After these expressions and the stresses in terms of the strain energy density function are introduced into the equilibrium equation we obtain an ordinary differential equation for p:

$$\frac{dp}{d\lambda} = \beta \frac{W^*_{,\lambda_\theta} - W^*_{,\lambda_r}}{\beta\lambda - \mu\lambda^3} - \frac{dW^*_{,\lambda_r}}{d\lambda} \tag{30}$$

subject to the boundary conditions

$$p(R_i) = p_i \ , \tag{31}$$

$$p(R_e) = 0 \ . \tag{32}$$

Isotropic blood vessels A blood vessel generally exhibit anisotropic behavior when subjected to large variations in internal pressure and distending force. When the degree of anisotropy is small, the blood vessel may be treated as isotropic. For isotropic materials it is convenient to introduce the strain invariants:

$$I_1 = \lambda_r^2 + \lambda_\theta^2 + \lambda_z^2 \ , \tag{33}$$

$$I_2 = \lambda_r^2\lambda_\theta^2 + \lambda_\theta^2\lambda_z^2 + \lambda_z^2\lambda_r^2 \ , \tag{34}$$

$$I_3 = \lambda_r^2\lambda_\theta^2\lambda_z^2 \ . \tag{35}$$

These are measures of strain that are independent of the choice of coordinates. If the material is incompressible,

$$I_3 = j^2 \equiv 1 \ , \tag{36}$$

and the strain energy density is a function of the first two invariants,

$$W = W(I_1, I_2) \ . \tag{37}$$

The least complex form for an incompressible material is the first–order polynomial, which was first proposed by Mooney to characterize rubber,

$$W^* = \frac{G}{2}\left[(I_1 - 3) + k(I_2 - 3)\right] \ . \tag{38}$$

It involves only two elastic constants. A special case, where $k = 0$, is the neo–Hookean material, which can be derived from thermodynamics principles for a simple solid. Exact solutions can be obtained for the cylindrical deformation of a thick–walled tube. In the case where there is no residual strain, we have the following:

$$p = -G(1 + k\mu^2)\left[\frac{\log\lambda}{\mu} + \frac{1}{2\mu^2\lambda^2}\right] + c_0 \ , \tag{39}$$

$$\sigma_r = G\left[\frac{1}{\lambda^2\mu^2} + k\left(\frac{1}{\mu^2} + \frac{1}{\lambda^2}\right)\right] + p \ , \tag{40}$$

$$\sigma_\theta = G\left[\lambda^2 + k\left(\frac{1}{\mu^2} + \lambda^2\mu^2\right)\right] + p \ , \tag{41}$$

$$\sigma_z = G\left[\mu^2 + k\left(\lambda^2\mu^2 + \frac{1}{\lambda^2}\right)\right] + p \ . \tag{42}$$

$$\tag{43}$$

However, these above equations predict stress softening for a vessel subjected to internal pressurization at fixed lengths, rather than the stress stiffening observed in experimental studies on arteries and veins (see Figs. 4 and 5).

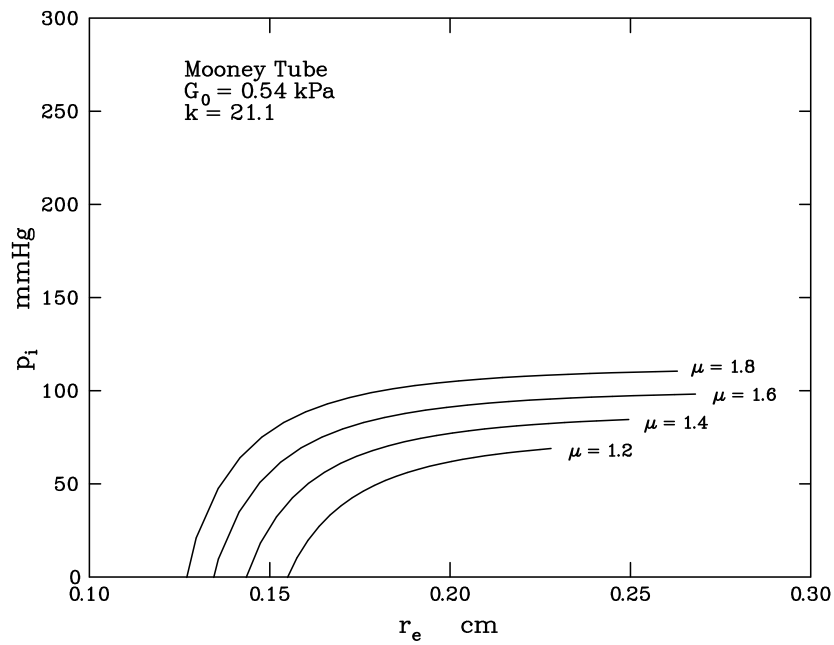

Figure 4: Pressure–radius curves for a Mooney–Rivlin tube with the approximate dimensions of the carotid

An alternative isotropic strain energy density function which can predict the appropriate type of stress stiffening for blood vessels is an exponential where the argument is a polynomial of the strain invariants. The first–order form is given by

$$W^* = \frac{G_0}{2k_1} \exp\left[k_1(I_1 - 3) + k_2(I_2 - 3)\right] \ . \tag{44}$$

This requires the determination of only two independent elastic constants. The third, G_0, is introduced to facilitate scaling of the argument of the exponent (see Figs. 6 and 7). This exponential form is attractive for several

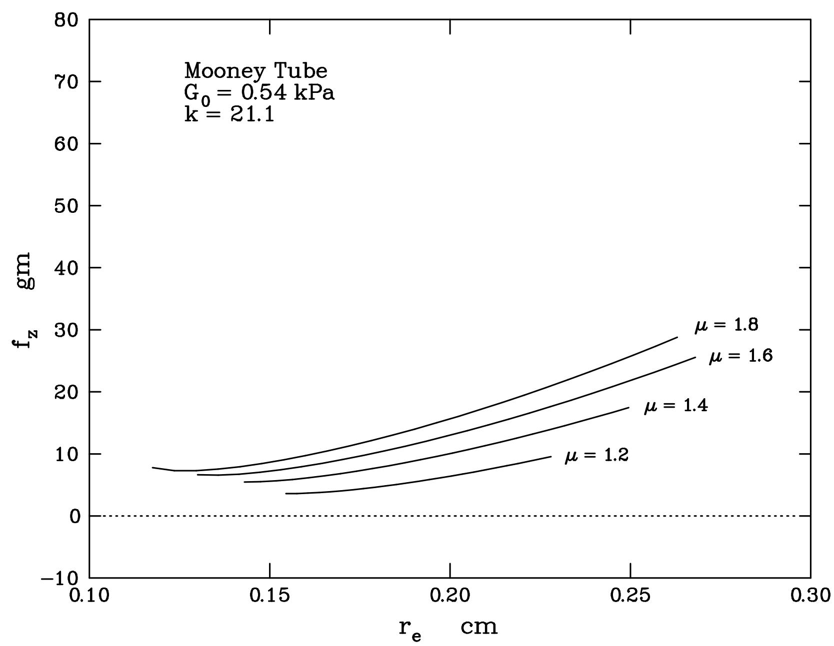

Figure 5: Longitudinal distending force as a function of radius for the Mooney–Rivlin tube

reasons. It is a natural extension of the observation that biological tissues stiffness is proportional to the load in simple elongation. This stress stiffening has been attributed to a statistical recruitment and alignment of tangled and disorganized long chains of proteins. The exponential forms resemble statistical distrubutions derived from these same arguments.

Anisotropic blood vessels. Studies of the orthotropic behavior of blood vessels may employ polynomial or exponential strain energy density functions that include all strain terms or extension ratios. In particular, the strain energy density function can be of the form

$$W^* = q_n(\lambda_r, \lambda_\theta, \lambda_z) \tag{45}$$

or

$$W^* = e^{q_n(\lambda_r, \lambda_\theta, \lambda_z)} \ , \tag{46}$$

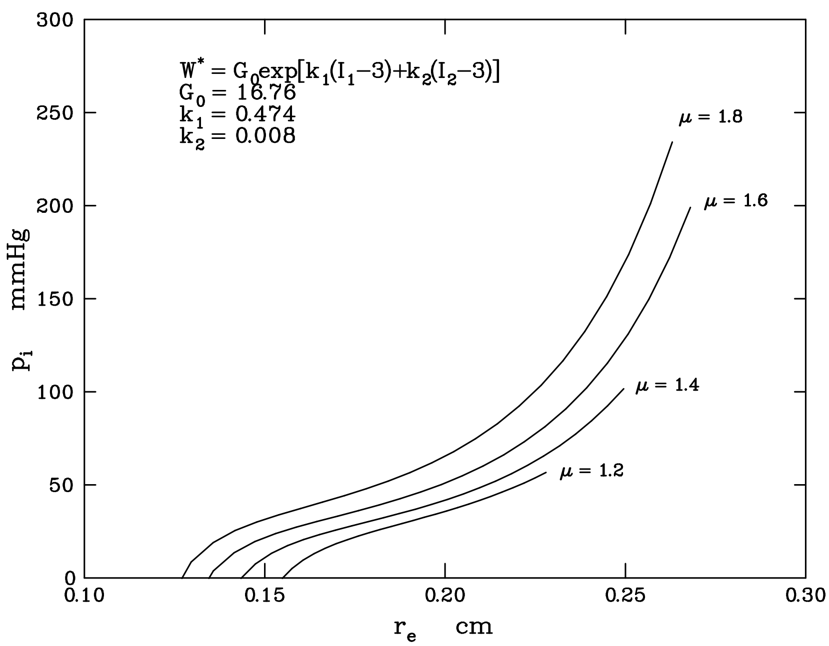

Figure 6: Pressure–radius curves for tube with the approximate dimensions of the carotid calculated using an isotropic exponential strain energy density function

where q_n is a polynomial of order n. Since the material is incompressible, the explicit dependence upon λ_r can be eliminated either by substituting $\lambda_r = \lambda_\theta^{-1}\lambda_z^{-1}$ or by assumping that the wall is thin and hence that the contribution of these terms is small.

Care must be taken to formulate expressions that will lead to stresses that behave properly. For this reason it is convenient to formulate the strain energy density in terms of the Lagrangian strains,

$$e_i = \frac{1}{2}(\lambda_i^2 - 1) , \tag{47}$$

and in this case we can consider polynomials of the lagrangian strains, $q_n(e_r, e_\theta, e_z)$.

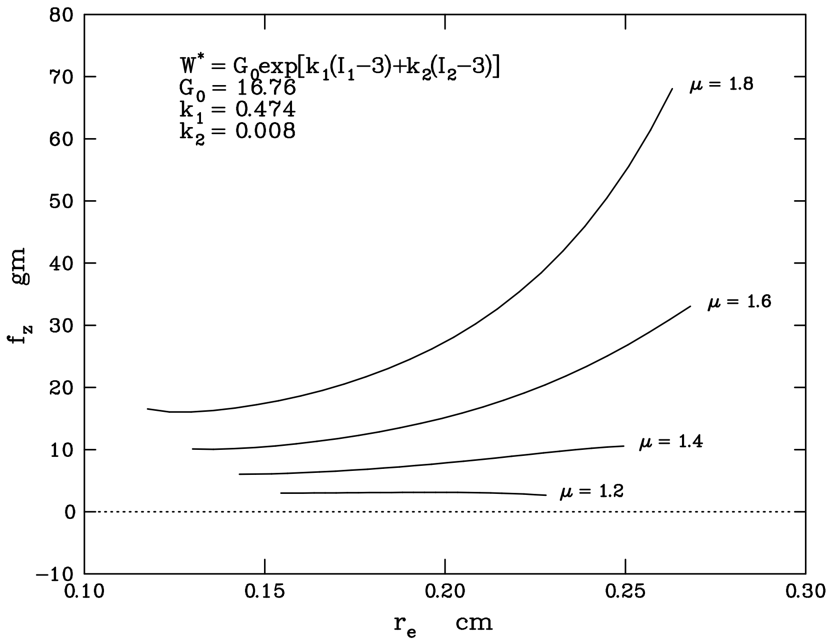

Figure 7: Longitudinal distending force as a function of radius for the isotropic tube

Vaishnav et al. [15] proposed using a polynomial of the form

$$W^* = \sum_{i=2}^{n} \sum_{j=0}^{i} a_{i\ j-i} e_\theta^{i-j} e_z^{j} \tag{48}$$

to approximate the behavior of the canine aorta. They found better correlation with order–three polynomials over order–two, but order–four polynomials did not warrant the addition work.

Later, Fung et al. [10] found very good correlation with an expression of the form

$$W = \frac{C}{2} \exp\left[a_1(e_\theta^2 - e_z^{*2}) + a_2(e_z^2 - e_z^{*2}) + 2a_4(e_\theta e_z - e_\theta^* e_z^*)\right] \tag{49}$$

for the canine carotid artery, where e_θ^* and e_z^* are the strains in a reference configuration at in situ length and pressure. Why should this work? One

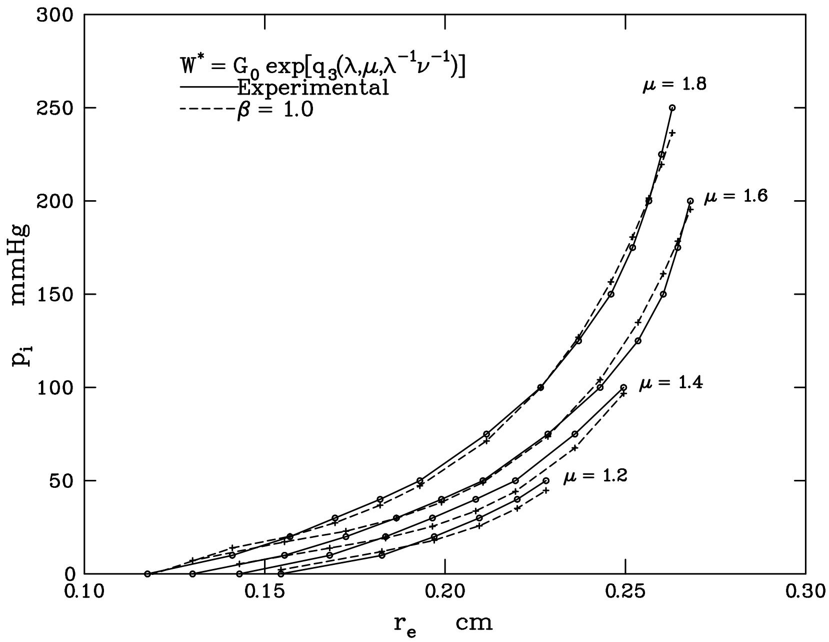

Figure 8: Pressure–radius curves for a fully orthotropic vessel calculated with an exponential strain energy density function

answer appears to be related to residual stresses and strains.

When residual stresses are ignored, large–deformation analysis of thick–walled blood vessels predicts steep distributions in σ_θ and σ_z through the vessel walli, with the highest stresses at the interior. This prediction is considered significant because high tensions in the inner wall could inhibit vascularization and oxygen transport to vascular tissue.

When residual stresses are considered, the stress distributions flatten considerably and become almost uniform at in situ length and pressure. Figure 10 shows the radial stress distributions computed for a vessel with $\beta = 1$ and $\beta = 1.11$. Takamizawa and Hayashi have even considered the case where the strain distribution is uniform in situ [13]. The physiological implications are that vascular tissue is in a constant state of flux. New tissue is synthesized in a state of stress that allows it to redistribute the internal

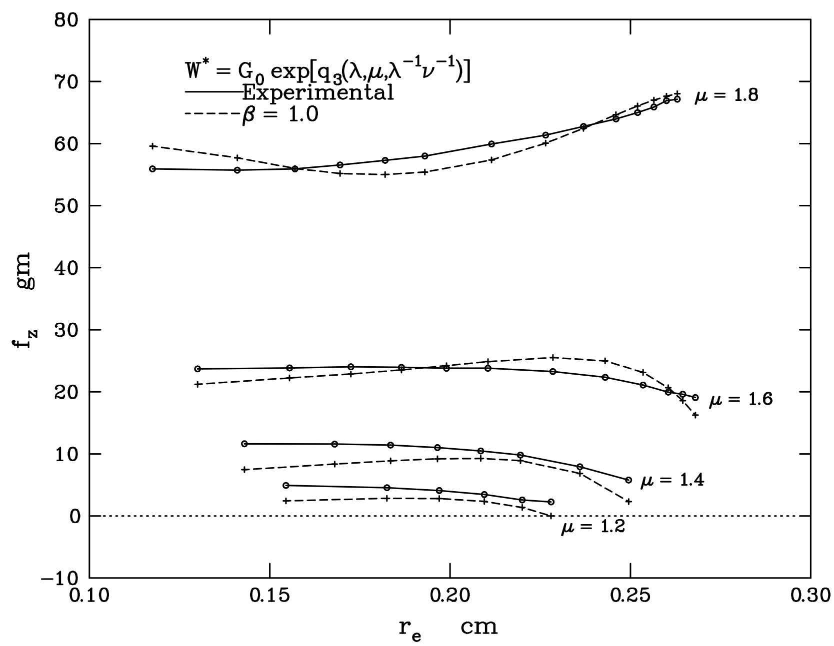

Figure 9: Longitudinal distending force as a function of radius for the orthotropic vessel

loads more uniformly. There probably is no stress–free reference state [8], [11], and [12]. Continuous dissection of the tissue into smaller and smaller pieces would continue to relieve residual stresses and strains [14].

*Work sponsored by the U.S. Department of Energy under Contract W-31-109-Eng-38.

References

[1] Bergel, D. H., 'The static elastic properties of the arterial wall', J. Physiol., London, 156: 445–457, 1961.

[2] Carew, T. E., Vaishnav, R. N., and Patel, D. J., 'Compressibility of the arterial walls', Circ. Res., 23: 61–68, 1968.

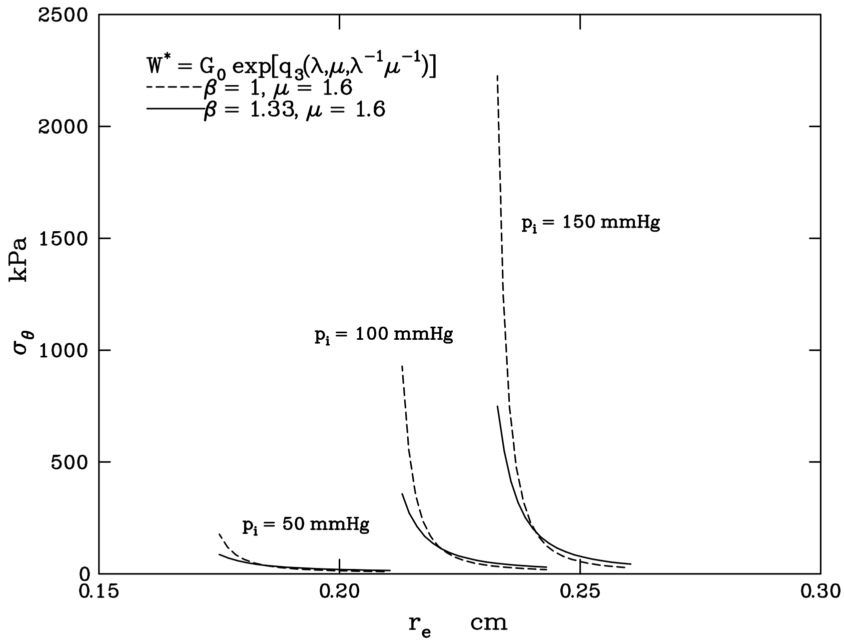

Figure 10: Stress distributions through the wall at various pressures for the orthotropic vessel

[3] Chu, B. M., and Oka., S., 'Influence of longitudinal tethering on the tension in thick–walled blood vessels in equilibrium', Biorheol., 10: 517–525, 1973.

[4] Choung, C. J., and Fung, Y. C., 'On residual stresses in Arteries', ASME J. of Biomed. Engrg, 108: 189–192, 1986.

[5] Dobrin, P. B., 'Mechanical properties of arteries', Physiol. Rev., 58: 397–460, 1978.

[6] Dobrin, P. B., and Canfield, T. R., 'Elastase, collagenase, and the biaxial elastic properties of dog carotid artery', Am. J. Physiol., 2547: H124–H131, 1984.

[7] Dobrin, P. B., and Rovick, A. A., 'Influence of vascular smooth muscle on contractile mechanics and elasticity of arteries', Am. J. Physiol., 217: 1644–1651, 1969.

[8] Dobrin, P. D., Canfield, T., and Sinha, S., 'Development of longitudinal retraction of carotid arteries in neonatal dogs', Experientia 31: 1295–1296, 1975.

[9] Doyle, J. M. and Dobrin, P. B., 'Finite deformation the relaxed and contracted dog carotid artery', Microvasc. Res., 3: 400–415, 1971.

[10] Fung, Y. C., Fronek, K., and Patitucci, P., 'Pseudoelasticity of arteries and the choice of its mathematical expression', Am J. Physiol., 237: H620–H631, 1979.

[11] Fung, Y. C., Liu, S. Q., and Zhou, J. B., 'Remodeling of the constitutive equation while a blood vessel remodels itself under strain', J. Biomech. Engrg., Trans. of the ASME, 115: 453–459, 1993.

[12] Rachev, A., Greenwald, S., Kane, T., Moore, J., and Meister, J.–J., 'Effects of age–related changes in the residual strains on the stress distribution in the arterial wall', Proc. Thirteenth S. Biomed. Engrg. Conf., Biomed. Engrg. Rec. Devel., J. Vassougi ed., U. of Dist. Columbia, Washington D. C., 409–412, 1994.

[13] Takamizawa, K. and Hayashi, K., 'Strain energy density function and the uniform strain hypothesis for arterial mechanics', J. Biomech., 20: 7–17, 1987.

[14] Vassoughi, J., 'Longitudinal residual strain in arteries', Proc. of the 11th South. Biomed. Engrg. Conf., Memphis, TN, October, 1992.

[15] Vaishnav, R. N., Young, J. T., Janicki, J. S., and Patel, D. J., 'Non–linear anisotropic elastic properties of the canine aorta', Biophys. J., 12: 1008–1027, 1972.

[16] Vaishnav, R. N., and Vassoughi, J.,'Estimation of residual stresses in aortic segments', **Biomedical Engineering II**, Recent Developments, Hall, C.W., ed., Pergamon Press, 330–333, 1983.

[17] Von Maltzahn, W.–W., Desdo, D., and Wiemier, W., 'Elastic properties of arteries: a nonlinear two–layer cylindrical model', J. Biomech., 4: 389–397, 1981.

[18] Wolinsky, H., and Glagov, S., 'Comparison of abdominal and thoracic aortic media structure in mammals', Circ. Res., 25: 677–686, 1969.